Local and Average Structure of Lead Titanate Based Ceramics

J. Frantti , S. Ivanov , J. Lappalainen , S. Eriksson , V. Lantto , S. Nishio , M. Kakihana & H. Rundlöf

Local and Average Structure of Lead Titanate Based Ceramics

J. FRANTTI,[†][§] S. IVANOV,[¶] J. LAPPALAINEN,[‡] S. ERIKSSON,[§]
V. LANTTO,[‡] S. NISHIO,[†] M. KAKIHANA,[†] and H. RUNDLÖF[§]

[†]*Materials and Structures Laboratory, Tokyo Institute of Technology, 4259 Nagatsuta, Midori-ku, Yokohama, 226-8503 Japan*
[¶]*X-Ray Laboratory, Department of Inorganic Materials, Karpov Institute of Physical Chemistry, 103064, ul. Vorontsovo pole, 10 Moscow, Russia*
[‡]*Microelectronics and Materials Physics Laboratories, University of Oulu, Linnanmaa, P.O. Box 4500, FIN-90014 University of Oulu, Finland*
[§]*Studsvik Neutron Research Laboratory, Uppsala University, S-61182, Nyköping, Sweden*

The revised lattice dynamics of $Pb(Zr_xTi_{1-x})O_3$ (PZT) with $0.10 \leq x \leq 0.54$ ceramics is reported. The phase transition from tetragonal phase to the monoclinic phase is proposed to occur *via* locally distorted regions. Neutron diffraction data suggests that these local regions transform to the monoclinic phase with decreasing temperature, when $x \approx 0.50$.

1. INTRODUCTION

The structural details of $Pb(Zr_xTi_{1-x})O_3$ (PZT) ceramics have been revised during the last few years. Particularly lead zirconate and high-Zr-content PZT have been studied extensively by transmission electron microscopy (see, for example Refs. [1–3]) and neutron diffraction (see Ref. [4] and references cited therein). These studies indicated that the local symmetry is broken, as superlattice reflections were observed in electron diffraction patterns. These reflections should be systematically absent according to the $R3c$ space group symmetry, and they were not observed by x-ray or neutron diffraction [3, 4].

[§]To whom correspondence should be addressed (jfrantt1@rlem.titech.ac.jp)

There are three possible mechanisms for the generation of superlattice reflections in perovskite diffraction patterns [5]: chemical ordering between cation species, octahedral tilts and antiparallel displacement of cations. Viehland related the presence of these superlattice reflections to the locally ordered oxygen tilts [1]. Ricote et al. studied PZTs with $0.55 \leq x \leq 0.94$ and they proposed a model, where antiparallel displacements of cations was proposed to be the origin of the superlattice reflections [3]. There has not been any observations of cation ordering in PZTs (to our knowledge), in accordance with recent theoretical studies [6–8]. These calculations explain, why there occurs ordering in many heterovalent solid solutions (such as in the case of well known relaxor material $Pb(Mg_{1/3}Nb_{2/3})O_3$, (PMN), where the nominal charges of the B cations are $+2$ and $+5$, for Mg and Nb, respectively), but never for the homovalent solid solutions, such as PZT ceramics (where the B cations have the same nominal charge $+4$). The explanation is based on electrostatic interactions among different B cations, and gives a rather simple explanation for the experimental results. On the other hand, the effect of La (2 at%) on the antiferroelectric phase transitions in PZTs with $x = 0.95$ was studied by Xu et al. [9]. They reported La-induced incommensuration in this antiferroelectric orthorhombic PZT. The phase transition, which was reported to be diffuse in nature, occurred at about $210°C$ from a ferroelectric structure when cooled from above [9].

Quite recently, El Marssi et al. [10] used Raman spectroscopy to study tetragonal and trigonal, La-modified PZT (PLZT) ceramics. They found that the Raman selection rules (RSR) in multidomain ferroelectric PLZT ceramics were not obeyed. They further found a loss of RSR in micro-Raman measurements (laser beam spot size $\approx 2\mu m$) for both trigonal and tetragonal PZTs and nonrelaxor trigonal PLZT ceramics, and concluded that the lack of RSR means that ceramic is in a multidomain state. Interestingly, they found that the selection rules were obeyed in the case of relaxor PLZTs, and explained it to be due to the second-order Raman process. Their work [10, 11] shows how Raman spectroscopy can be used as a powerful method to obtain complementary information for the electrical measurements and diffraction experiments, in the case of PZTs and PLZTs.

It was found that the symmetry of the tetragonal PZTs with $0.10 \leq x \leq 0.20$ was lowered [12] from the tetragonal one at low temperatures, at least in a local level. This was concluded from the split E-symmetry modes in Raman spectra. Later, Noheda et al. [13] reported a phase transition from the tetragonal phase to the monoclinic phase for $x = 0.52$. The study of PZTs with $0.10 \leq x \leq 0.54$ showed that the frequency difference between the split E-symmetry modes was increasing with increasing x [14]. Interestingly,

the frequency difference between the $E \oplus B_1$ modes in PZTs (which are degenerate in $PbTiO_3$) showed a frequency jump of roughly 6 cm^{-1}, when x increased from 0.40 to 0.50. This was related to the phase transition from the tetragonal symmetry to the monoclinic symmetry [14]. In order to find out, whether this symmetry breaking is local or if it is due to the change in the average space symmetry, a series of neutron diffraction experiments were carried out [15] as a function of x, for the same samples which were used in our previous Raman studies [12, 14]. It was found, on similar lines as Noheda et al. [16] found for their $Pb(Zr_{0.52}Ti_{0.48})O_3$ sample that lead ions are markedly displaced from their ideal positions in the $\langle 110 \rangle$ direction. However, it was also found that the fractional coordinates of the Zr and Ti ions differed, and that they were likely shifted in the $\langle 110 \rangle$ direction as well [15]. Noheda et al. [16] interpreted that the phase transition from the tetragonal phase to the monoclinic phase is due to the condensation of the local Pb displacements in the tetragonal phase along one of the $\langle 110 \rangle$ directions. However, neutron and synchrotron diffraction experiments do not tell to which extent these displacements are static and dynamic. It is not probable that all the lead ions occupy same crystallographic site, and due to the misplaced lead ions there are lower symmetry regions in a tetragonal matrix, as will be discussed below.

The studies carried out for the tetragonal PZTs are not so extensive as the ones carried out for the trigonal PZTs. In this paper we concentrate on the tetragonal PZTs, and review the structural data available for these compositions. Occasionally, we present some new measurement data. We will first discuss the structural features of PZTs (i.e., homovalent B-cation substitution for titanium in lead titanate), after which the case of neodymium and lanthanum modified lead titanates (heterovalent substitution for lead) is discussed. Roughly speaking, diffraction techniques are categorized as means to obtain average structure and Raman spectroscopy is used as a probe to study the local deviations from this average. As the role of the A_1-symmetry modes, and particularly the role of the $A_1(1TO)$ mode is significant for the ferroelectricity, we discuss it rather extensively. We also outline the experiments to be carried out, and correct some misidentified modes in our previous reports.

2. EXPERIMENTAL

The sample preparation of ceramic $Pb(Zr_xTi_{1-x})O_3$ and $Pb_{1-3y/2}Nd_yTiO_3$ (PNT) samples is described in our previous articles [12, 14, 15, 17, 18].

The $Pb_{0.85}La_{0.10}TiO_3$ (PLT) sample was prepared in an analogous way as $Pb_{0.85}Nd_{0.10}TiO_3$ sample, using conventional solid-state reaction technique.

Raman spectra were collected at room temperature using Jobin Yvon T64000 spectrometer model and visible range (457.935, 487.986, and 514.532 nm) laser light. The laser output powers in the visible range wavelengths were 1.0 mW (457.935 nm) and 2.5 mW (487.986 and 514.532 nm). Low-temperature measurements were carried out using a power of 50 μW and an excitation wavelength of 514.532 nm. The resolution of the Raman spectrometer was about 1 cm^{-1}.

Constant wavelength data was measured at the Studsvik Neutron Research Laboratory. Data sets were collected at room temperature and at 10 K. The wavelength was 1.47Å, the two-theta range measured was from 4.00 to 139.92° with a step size of 0.08° and the scanning time was 12 hours. We also refer to the POLARIS and HRPD time-of-flight neutron diffraction instruments (both at ISIS). For more details, see Ref. [15]. Rietveld refinements were carried out using the General Structure Analysis System (GSAS) [19]. It should be noted that the estimated standard errors given below for the lattice constants and other structural parameters are probably too small, as is typical for Rietveld refinement, and should be adopted with caution.

The Second Harmonic Generation (SHG) technique (Nd:YAG laser) was used as a sensitive and reliable method for establishing the presence or absence of a center of symmetry.

3. RESULTS AND DISCUSSION

3.1. Neutron Diffraction Studies

Previous time-of-flight neutron diffraction experiments carried out at the Rutherford Appleton Laboratory at ISIS using POLARIS (a medium-resolution, high-intensity powder diffractometer) and HRPD (high-resolution powder diffractometer) instruments showed that PZT with $0.52 \leq x \leq 0.54$ has an average symmetry *Cm* at room temperature and at low-temperature [15]. We made additional refinements for the constant wavelength data collected from the $Pb(Zr_{0.50}Ti_{0.50})O_3$ sample at room temperature and at 10 K, using both the tetragonal (*P4mm*) and monoclinic (*Cm*) space group symmetries. Results are summarized in Table I. During the refinements, either the *z* ordinate of lead or Zr/Ti cation was fixed. Also space groups *Pmm*2 (with *a* and *b* axes parallel to the tetragonal *a* and *b* axes and a second setting with *a* and *b* axes rotated by 45° relative to the tetragonal *a* and *b* axes), *P*4 and *Cm* were previously used in the refinements

TABLE I Details of structure refinements for the $Pb(Zr_{0.50}Ti_{0.50})O_3$ sample (carried out using GSAS software [19]). Data was collected at room temperature and at 10 K using the constant-wavelength diffractometer at Studsvik. To see find out the probable space group we compared the statistical parameters of the tetragonal $P4mm$ (one formula unit per primitive cell) and monoclinic Cm (two formula units per unit cell) space groups. For comparison, we represent (from Ref. [15]) the refinement results for the data collected from the same sample at room temperature using a POLARIS instrument. During the refinements, the z ordinate of either Pb or Zr/Ti cation(s) was fixed, and that ordinate is typed here using a bold font

	POLARIS $T = 295$ K $P4mm$	STUDSVIK $T = 295$ K $P4mm$	$T = 295$ K Cm	$T = 10$ K $P4mm$	$T = 10$ K Cm
a (Å)	4.030341(34)	4.02988(10)	5.69954(33)	4.02077(12)	5.6892(4)
b (Å)	4.030341(34)	4.02988(10)	5.69871(33)	4.02077(12)	5.6839(4)
c (Å)	4.14490(7)	4.14563(19)	4.14554(19)	4.15521(23)	4.15523(21)
β (°)	90	90	90.066(22)	90	90.266(10)
U_{11}(Pb) (Å^2)	—	—	0.0255(17)	—	0.0139(13)
U_{22}(Pb) (Å^2)	—	—	0.0300(19)	—	0.0160(14)
U_{33}(Pb) (Å^2)	—	—	0.0186(11)	—	0.0084(9)
U_{13}(Pb) (Å^2)	—	—	0.0222(17)	—	0.0149(14)
U_{iso}(Pb) (Å^2)	0.01349(34)	0.0131(5)	—	0.0023(4)	—
U_{iso}(Ti, Zr) (Å^2)	0.0050(5)	0.0041(20)	0.0031(19)	0.0074(22)	0.0045(19)
U_{iso}(O$_1$) (Å^2)	0.01537(33)	0.0186(9)	0.0141(9)	0.0157(9)	0.0075(8)
U_{iso}(O$_{2,3}$)	0.01457(22)	0.0144(5)	0.0127(5)	0.0140(5)	0.0095(5)
x(Pb) $= y$(Pb)	0.0240(5)	0.0236(10)	0	0.0201(8)	0
z(Pb)	0.0000(7)	0.0000(7)	0	0.0000(7)	0
x(Zr)	0.5	0.5	0.495(5)	0.5	0.4759(29)
x(Ti)	0.5	0.5	0.495(5)	0.5	0.4759(29)
y(Zr)	0.5	0.5	0	0.5	0
y(Ti)	0.5	0.5	0	0.5	0
z(Zr)	**0.5649**	**0.5638**	0.5680(12)	**0.582**	0.5846(13)
z(Ti)	**0.5649**	0.5676(21)	0.5748(26)	0.5927(25)	0.6079(34)
x(O$_1$)	0.5	0.5	0.4801(18)	0.5	0.4683(12)
y(O$_1$)	0.5	0.5	0	0.5	0
z(O$_1$)	0.0921(7)	0.0907(10)	0.0894(10)	0.0954(10)	0.0956(9)
x(O$_{2,3}$)	0.5	0.5	0.2386(38)	0.5	0.2239(12)
y(O$_{2,3}$)	0	0	0.2488(15)	0	0.2465(10)
z(O$_{2,3}$)	0.6110(7)	0.6092(7)	0.6095(7)	0.6163(8)	0.6183(7)
χ^2	3.263	1.922	1.885	2.602	2.110
R_{wp} (%)	2.36	6.00	5.93	6.91	6.21
R_p (%)	4.45	4.49	4.42	5.37	4.74

to model PZTs with $0.20 \leq x \leq 0.54$, in addition to the *P4mm* space group, see discussion in Ref. [15]. The result was that at room temperature *P4mm* space group gave the best fit for the $0.20 \leq x \leq 0.50$ samples, and *Cm* gave the best fit for the $0.52 \leq x \leq 0.54$ samples (which were modeled using two phases, *Cm* and *P4mm*, see Ref. [15]. Refinements using the trigonal low- or high-temperature phase as a secondary phase and tetragonal or monoclinic phase as a first phase were carried out. It was found that among these two-phase models the combination of monoclinic and tetragonal phases was the most satisfying for the description of the PZT system with $x \approx 0.52$ [15]). At low-temperature, the monoclinic phase was extended towards lower Zr contents, as Table I indicates. Thus, it can be concluded that the low-temperature phase of $Pb(Zr_{0.50}Ti_{0.50})O_3$ is monoclinic, although the monoclinic distortion at room temperature is small, and the room temperature structure is probably tetragonal. This is consistent with our previous Raman observations [14] stating that at 20 K the phase symmetry changes from tetragonal symmetry when x changes from 0.40 to 0.50. At room temperature, we found that $x = 0.52$ sample had 69% monoclinic and 31% tetragonal phase (refinements carried out for the HRPD and POLARIS data both revealed the same weight fractions), and $x = 0.54$ had 73% monoclinic and 27% tetragonal phase, in weight fractions. In the case of HRPD data, refinements proposed that the weight fraction of the monoclinic phase is 83% at 4.2 K. This suggests that the secondary phase, modeled here by tetragonal phase, transform to monoclinic phase with decreasing temperature. Although one cannot rule out the possibility that this second phase is nonstoichiometric and/or even amorphous, this result suggests that it is probably crystalline phase, as do our Raman results discussed below.

It should be noted that the lattice parameters obtained from the refinements carried out for the POLARIS data and Studsvik data differ. That is probably due to the different profile functions used for the TOF data and constant wavelength data. This is connected to the line shape problem discussed previously in Ref. [15].

3.2. Second Harmonic Generation Results

Table II summarizes the observed phase transition temperatures for three selected samples estimated from the Second-Harmonic-Generation (SHG) data. The data for the phase transition temperature to the cubic phase agrees well with the well-known phase diagram by Jaffe et al. [20], except the $x = 0.20$ sample, for which our sample had higher T_C. It became clear that SHG gives the T_C more reliably than Raman spectroscopy. This is since in the case of high-temperature Raman spectra one can observe Raman modes

TABLE II Phase transition temperatures T_C (corresponding to the phase transition $Pm3m \rightarrow P4mm$ for $Pb(Zr_x Ti_{1-x})O_3$ samples as estimated from the second harmonic generation data. In the case of $x = 0.54$, we also give tentatively a phase transition temperature between the monoclinic (Cm) and tetragonal phases ($P4mm$), although it has not yet confirmed for this sample

x	T_C (K)	T_1 (K)
0.20	748	—
0.50	676	—
0.54	673	399

even when the sample is nominally in a paraelectric cubic phase, where first-order Raman scattering is not allowed [18].

3.3. Raman Observations

3.3.1. Lead zirconate titanates. Raman measurements showed that the *E*-symmetry modes are split in PZTs with $0.10 \le x \le 0.51$ (for the higher Zr contents it is rather difficult to say if there are true *E*-symmetry modes, as the phase symmetry changes *via* monoclinic phase to the trigonal phase). This splitting was increasing with increasing x and decreasing temperature, see figures in Refs. [12, 14]. Noheda et al. [16] proposed that the phase transition from the tetragonal phase to the monoclinic phase is due to the condensation of the local Pb displacements in the tetragonal phase along one of the $\langle 110 \rangle$ directions. In tetragonal phase, the Brillouin zone center normal modes form the basis for the representation $4A_1 \oplus B_1 \oplus 5E$ (Raman active modes transform as the representation $3A_1 \oplus B_1 \oplus 4E$). Using the fact that the space group Cm (C_s^3) is a subgroup of $P4mm$ (C_{4v}^1) it can be seen that we have the following relationships between the irreducible representations of the point groups C_{4v} and C_s: $A_1 \rightarrow A'$, $B_1 \rightarrow A''$, and $E \rightarrow A' \oplus A''$. Thus, the Raman active modes in the monoclinic phase transform as $7A' \oplus 5A''$. As the *E*-symmetry modes are split far before the phase transition occurs, one must take seriously the possibility that PZT ceramics contain locally distorted crystalline regions, and once the number of these regions increases phase transition takes its place. We assume that these regions are crystalline, as the peaks observed at low-temperature have small half-width-at-half-magnitude (HWHM) values, and the spectrum can be considered as a distorted form of a tetragonal Raman spectrum.

Our previous neutron diffraction study [15] showed that the *average* displacement of lead ions in the $\langle 110 \rangle$ direction increases with increasing

Zr content. This phenomenon was accompanied by the difference $\Delta = z(\text{Ti}) - z(\text{Zr})$ between the fractional z-coordinates of the Ti and Zr ions. Interestingly, Δ was negative for small values of x, roughly zero for $x \approx 0.50$ and positive for the higher values of x. As the splitting of E-symmetry modes was observed to increase monotonically with increasing x (and slightly with decreasing temperature), we conclude that the main reason for the peak split are misplaced lead ions. There was a frequency jump of 6 cm^{-1} in the frequency of the assumed B_1 modes, when x increased from 0.40 to 0.50. As the composition change was large, it is not possible to say, whether the phase transition is of second order or not. Space group Cm is a subgroup of the $P4mm$ and $R3m$ space groups, and thus one cannot exclude the possibility of a continuous phase transition.

In order to study the behavior of these split modes measurements under electric field at various temperatures are necessitated. Raman spectroscopy suits well for the study of the phase transitions induced by the electric field. This is since the high electric field necessitates, from the practical point of view, small sample dimensions, and thus the conventional diffraction techniques are ruled out, or at least are not so conveniently available. This is even more pronounced at low temperatures, where the experiments are to be carried out. It is expected that lead ions respond cooperatively to the electric field, and due to the ordering of these ions a phase transition to the monoclinic phase is assumed to occur. Such kind of experiment would likely explain, why many properties (piezoelectric coefficient, susceptibility, etc.) of PZTs are superior when compared to the Ba and Sr based perovskites, such as (Ba, Sr) (Zr, Ti)O$_3$ ceramics.

3.3.2. Rare earth modified lead titanates. In contrast to the case of PZTs (homovalent substitution of Ti by Zr), the substitution of lead by trivalent rare earths has an effect of creating vacancies. Recently, Jiang et al. [21] reported the effect of A-cation substitution for the B-site order in the case of PMN ceramics. They found that the degree of B-site order increases with trivalent La^{3+} doping, while it decreases with monovalent K$^+$ doping. This phenomenon was related to the reduction (trivalent doping) or enhancement (monovalent doping) of the charge imbalance effect. The narrowing of the highest frequency band of PMN ceramics by trivalent substitution is opposed due to the vacancies created in order to maintain the charge balance [21]. In contrast to the case of PMN, the changes in band widths of rare earth modified lead titanates can be understood by considering the effect of vacancies and mass and ionic radius difference between lead (which rare earths are substituting) and rare earth ions. Due to these two effects, the HWHM values of the E(1TO), E(2TO), and $E \oplus B_1$ modes of PNT samples were increasing with
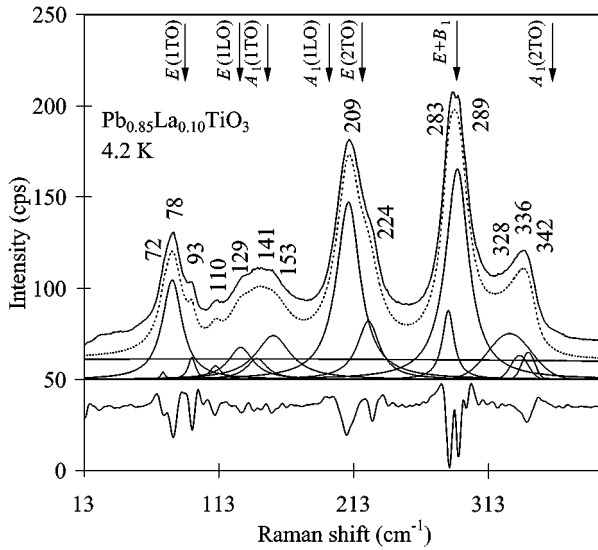
Figure 1. Low-frequency Raman spectra together with the curve fit measured from the $Pb_{0.85}La_{0.10}TiO_3$ sample at 4.2 K (local temperature ≈ 20 K). In order to see the shape of the measured Raman spectrum clearly, we shifted it up by 10 units. The dotted line is the fit. The curve at the bottom is the second derivative curve of the intensity and shows the splitting of the $E(2TO)$ and $E \oplus B_1$ modes. The positions of different Raman peaks at room temperature in $PbTiO_3$ (Ref. [25]) are also shown at the top.

increasing Nd concentration, so that the HWHM values of $Pb_{0.85}Nd_{0.10}TiO_3$ ceramics were roughly twice as large as the corresponding values of pure lead titanate powders [17]. Figure 1 shows the low-temperature (local temperature ≈ 20 K) Raman spectrum measured from the $Pb_{0.85}La_{0.10}TiO_3$ sample. The splitting of the $E(2TO)$ (asymmetrical line shape) and $E \oplus B_1$ modes is seen. This splitting indicates that the symmetry is broken in a local scale, as the previously made powder neutron and x-ray diffraction experiments between 10 and 1023 K did not reveal any phase transition for this material, except the diffuse one between the cubic ($Pm3m$) and tetragonal ($P4mm$) symmetries at around 565 K [22]. However, Rossetti et al. found a broadening of diffraction profiles, which they related to the local tetragonal distortion of the structure [22]. It has been reported previously that La-modified $PbTiO_3$ turns from the normal ferroelectric state (having micron sized domains) to the relaxor state containing polar nanodomains, when La content is 23 at.% [23]. This transformation occurs *via* tweed-line subdomain structures. Based
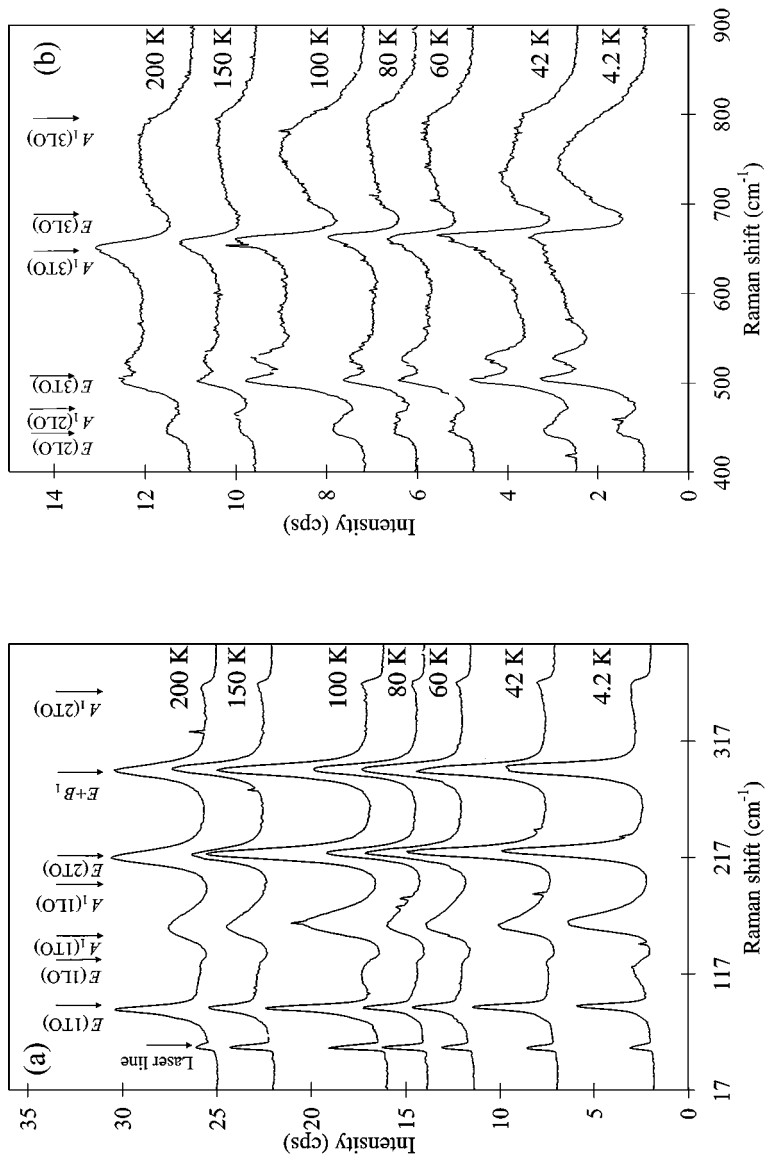
Figure 2. Low-temperature Raman spectra measured from the $Pb(Zr_{0.10}Ti_{0.90})O_3$ sample using excitation wavelength 457.935 nm. (a) Low-frequency spectra, (b) High-frequency Raman spectra. The positions of different Raman peaks at room temperature in $PbTiO_3$ (Ref. [25]) are also shown at the top.

on the phase diagram presented in Ref. [23] it is seen that $Pb_{0.85}La_{0.10}TiO_3$ is in a normal ferroelectric state at 20 K.

Several modes related to the electronic transitions at Nd-ions were found. For example, the mode at around $560 \, cm^{-1}$ in $Pb_{0.85}Nd_{0.10}TiO_3$ had such kind of origin (see Fig. 3 in Ref. [12]). In contrast, pure PZT samples (without Nd) have modes at around $570 \, cm^{-1}$, which is slightly unfortunate coincidence. Also the modes between 800 and $1000 \, cm^{-1}$ (see Fig. 5 in Ref. [17]) had the same origin. This was confirmed by measuring Raman spectra using different excitation wavelengths. There were also several other strong bands due to the electronic transitions at Nd ions at higher Raman shift area (the strongest bands were between 2200 and $3200 \, cm^{-1}$ and 4200 and $5000 \, cm^{-1}$, when the excitation wavelength was 514.532 nm).

3.4. Order-Disorder Versus Displacive Lattice Dynamics

There has been a lot of discussion, whether lead titanate has a displacive or order-disorder type phase transition. Previously it has been considered as a typical displacive ferroelectric, but the current view is different, as new experimental data became available (see, e.g., Ref. [24] and references cited therein). Nowadays, lead titanate and lead zirconate titanate are usually categorized as intermediate cases between these two extremes. This is largely related to the multiple potential well of lead ions, which is preserved also at high temperature (paraelectric phase) where the structure is, on the average, cubic. This further causes that the potential well corresponding to the soft mode has multiple minima at the cubic phase, which should be taken into account once one is analyzing the Raman spectra of lead titanate based ceramics.

Foster et al. [25] found that the anomalous line shape of the A_1(1TO) mode was due to the strong anharmonicity. In addition, the A_1-symmetry modes were found to be anharmonic in rare earth modified PZTs and lead titanates [17, 18]. In the case of A_1(1TO) mode one can use mean field theory to describe the intensities and frequencies of the subpeaks as a function of composition, temperature, and the laser beam wavelength used in the Raman experiments. It should be noted that this point of view assumes that the rigid oxygen octahedra is moving together with the B-cation against lead cage, and that it oscillates between two minima at elevated temperatures, also in the paraelectric phase. This is in contrast to the displacive ferroelectrics. However, this kind of model was necessitated in order to describe the observed subpeak structure of the A_1(1TO) mode, and the dynamic nature of the low-frequency background observed in PZTs (see Refs. [14, 18, 26]).
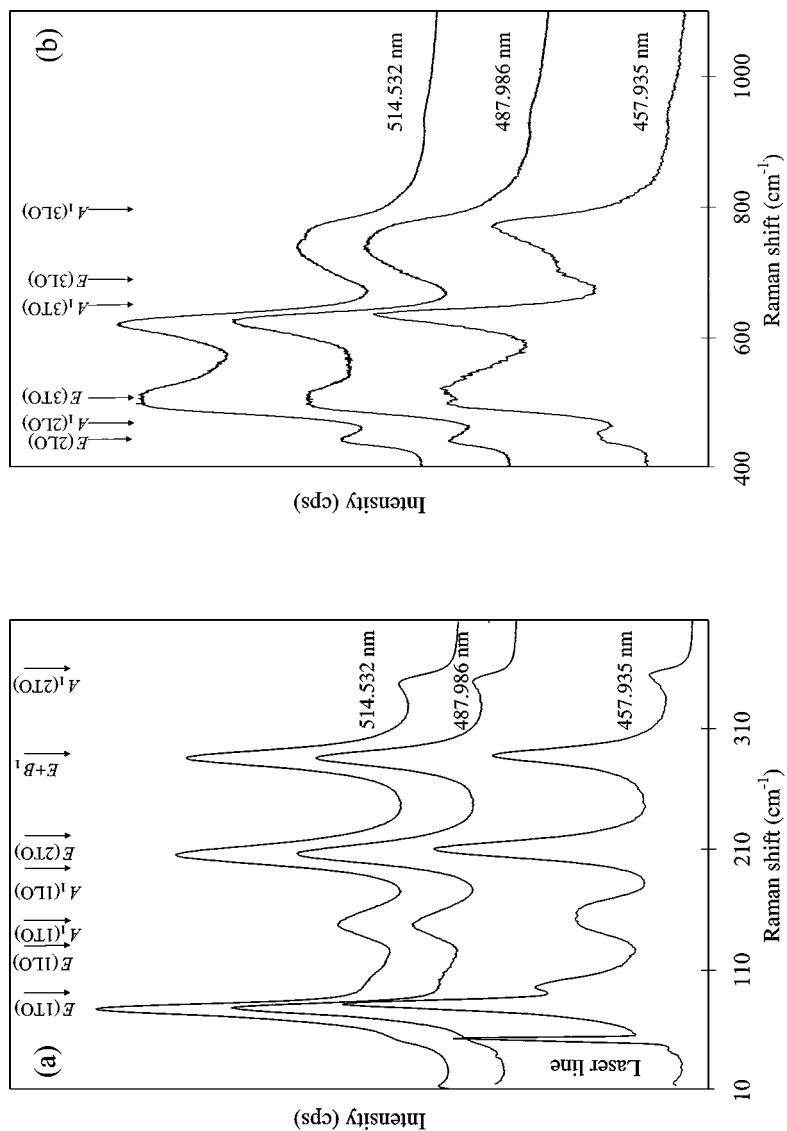
Figure 3. Raman spectra measured from the $Pb(Zr_{0.10}Ti_{0.90})O_3$ sample using several excitation wavelengths. (a) Low-frequency spectra, (b) High-frequency Raman spectra. The positions of different Raman peaks at room temperature in $PbTiO_3$ (Ref. [25]) are also shown at the top.
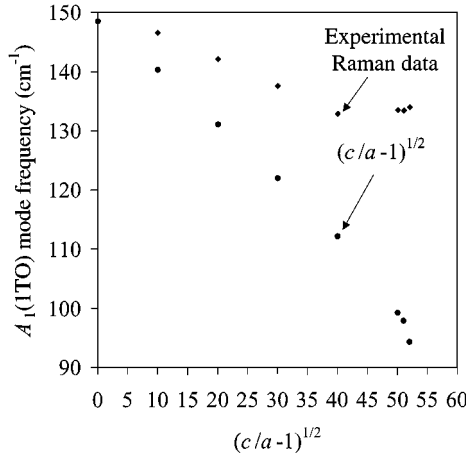
Figure 4. Frequency of the highest frequency subpeak of the $A_1(1TO)$ mode as a function of x. The data for $(c/a - 1)^{1/2}$ was obtained assuming that the polarization is proportional to the spontaneous strain.

We found previously [27] that the effect of Nd-doping is similar to the effect of temperature, i.e., the subpeak intensities were changing with increasing Nd-content in a similar way as with increasing temperature.

The changes of the relative intensities between subpeaks can be understood by considering the change of the linear term of the potential well. In mean field theory, linear term is directly proportional to the polarization and thus the linear term is a function of temperature. Burns and Scott [28] found that experimentally determinable "strain" c/a and spontaneous polarization fullfil the relations $P_s \propto \sqrt{c/a - 1}$ and $\omega(A_1(1TO)) \propto P_s$ rather well in the case of $PbTiO_3$ as a function of temperature. Basically, this relation could be used to qualitatively explain the effect of various dopants to the $A_1(1TO)$ mode frequency. We tested this relation previously in the case of Nd-modified lead titanates, and found that the discrepancy was rather large [17]. However, it offered a qualitative agreement between the $A_1(1TO)$ mode and strain (in the case of Nd-modified lead titanates, we found that the Nd addition decreases mainly the c axis, while the a axis was nearly constant [17]). Using the neutron diffraction data available for PZT at the room temperature from Ref. [15] (for $x = 0.20$, 0.30, 0.40 and 0.50) and X-ray diffraction data for $x = 0.51$ and $= 0.52$ samples (assuming they are tetragonal, which is actually not correct due to the monoclinic distortion) and taking the lattice parameters for lead titanate from Ref. [29], we

obtained the plot presented in Fig. 4. The constant for the experimental strain was selected so that it coincides with the value of the highest frequency subpeak of the A_1(1TO) mode of lead titanate (148.5 cm^{-1} [25]). The other frequency values were determined by curve fit from our PZT samples. The agreement is not a very good one, and fails for compositions $x \geq 0.50$. For the values close to the morphotropic phase it is not surprising, as the phase symmetry and polarization direction are changing. However, the agreement between the A_1(1TO) mode frequency and strain for tetragonal compositions ($0 \leq x \leq 0.40$) is comparable to the case of lead titanate (see Ref. [28], where the corresponding relationship is presented as a function of temperature).

The wavelength dependence is only seen, when interband transitions come into play. This is demonstrated in Fig. 3(a). Similarly, the polarization is diminished by the charge carriers generated by laser light (or by rare earth doping), and thus it is expectable, that the Raman spectra of the Pb(Zr$_{0.10}$Ti$_{0.90}$)O$_3$ sample measured using the 457.935 nm wavelength laser light should remind, as far as the subpeaks of the A_1(1TO) mode are concerned, the high-temperature Raman spectra or Raman spectra measured from PZT ceramics containing Nd, as is actually the case. Figure 2 shows the low-temperature Raman spectra measured from the Pb(Zr$_{0.10}$Ti$_{0.90}$)O$_3$ sample using an excitation wavelength of 457.935 nm.

The relative intensity of the A_1(3TO)-symmetry modes is strongly increasing with increasing laser light quanta energy, as Fig. 3(b) shows. The asymmetry of this mode is also increasing as the laser light quanta energy is increasing, which might be an indication of the interaction between the broad electronic continuum (conduction band) and these phonons. Also the behavior of A_1(3LO) mode is interesting, since its frequency and relative intensity have their maximum values, when the laser beam wavelength is 457.935 nm. This is probably related to the interaction between the light induced electron-hole pairs and longitudinal modes. The A_1(2LO) mode behaves in a similar manner; its frequency has a maximum when the laser beam wavelength is 457.935 nm. The frequencies of the E-symmetry modes have their maximum values at the excitation wavelength of 457.935 nm, but the effect is not so strong as it is in the case of the A_1-symmetry modes.

It is also worth noting that the E-symmetry modes are probably anharmonic. This is most probable at higher Zr concentrations, in the vicinity of the phase transitions. However, it is not possible to separate the A_1- and E-symmetry modes in the case of ceramics.

3.5. Structural Model

As the peak split of E-symmetry modes was increasing with increasing x and rare earth content y (and with decreasing temperature), we propose that there are lower symmetry regions, due to the misplaced lead ions, in tetragonal matrix. It is interesting to note that there is not a continuous change in the peak frequencies, but typically one can see two distinct peaks from the split of E-symmetry mode. This would hint that the polarization is changing rather rapidly once one moves from the locally distorted area to the tetragonal matrix. As the symmetry is decreased from the tetragonal $P4mm$ to the monoclinic symmetry Cm, the four-fold rotation axis is lost, and the only remaining mirror plane is the one containing the a and c axes. The symmetry lowering means that the polarization vector can be anywhere in the mirror plane. Bellaiche et al. [30] suggested that the polarization is changed in a continuous manner from the pseudocubic [001] direction to the pseudocubic [111] direction. They carried out computations for PZT system using a model, which takes compositional degrees of freedom into account. This model was able to predict the phase transition sequence from the tetragonal phase to the high-temperature trigonal phase *via* the monoclinic phase. This emphasizes how important it is to include local distortions for the computation of total energy, and is clearly a step towards more realistic calculations. Their model did not include octahedral-tilting degrees of freedom, from which they concluded that the oxygen tilts are not the driving force for the transition to the monoclinic phase. However, these locally distorted regions seem to have a lower symmetry, as our Raman data suggests, and it may not be adequate to describe PZTs as a one-phase system, but the description using a two-phase model is probably necessary. High-resolution electron microscopy studies are necessary for the direct observation of such kind regions. It should be emphasized that also diffraction experiments support this view, as the HWHM values of the XRD and neutron diffraction peaks of the $(h00)$ and $(0k0)$ reflections increase relative to the $(00l)$ reflections with increasing Zr content. In the vicinity of the morphotropic phase region it was necessary to use two-phase model in the Rietveld refinements [15, 16]. Further, it is not yet experimentally verified, whether the polarization vector changes in a continuous way as a function of Zr content. This might be affected even by the sample preparation technique, as the monoclinic phase is considered to be due to the condensation of the misplaced lead ions to one preferred direction (e.g., condensation along one of the $\langle 110 \rangle$ directions in the case of the phase transition from the tetragonal to the monoclinic phase) [16]. However, we stress that the phase transition from the average tetragonal

phase to the monoclinic phase can hardly be described as an ideal one involving only one crystal symmetry for one average composition. This would mean that the effect of the local composition fluctuation is so strong that it leads to the segregation of low-symmetry regions, which transform to monoclinic phase within the morphotropic phase compositions. The secondary phase has also been found by Noheda et al. [16] and might be unavoidable. Further, it is difficult (and to some extent irrelevant) to assign space group symmetry to these local areas.

The entropy of the phase transition is experimentally determined by measuring the temperature dependence of heat capacity over a sufficiently wide temperature range. If the randomly shifted lead ions "choose" one preferred $\langle 110 \rangle$ direction as the phase transition from the tetragonal phase to the monoclinic phase occurs, one should see a discontinuous change of entropy. We are working on this subject.

4. CONCLUSIONS

Structural features of lead titanate based ceramics were described. A view, where phase transition as a function of temperature and composition occurs via locally distorted crystalline regions present in the tetragonal matrix was proposed. It was pointed out that many features of lead titanate based ceramics are not consisted with the idea of displacive ferroelectrics, but an order-disorder description must be taken into account. Further, a lack of a model taking these locally distorted regions into consideration is probably one reason why it is difficult to obtain realistic theoretical estimates for various structural properties of lead titanate based ceramics. We suggest that one should take two-phase coexistence into account for the realistic description of the behavior of PZT ceramics as a function of composition and temperature. The phase transition from the tetragonal phase to the monoclinic phase was assumed to occur via these local crystalline regions, as the Raman and neutron diffraction data was suggesting. The total volume of these local areas is increasing with increasing Zr content as the morphotropic phase is approached from the Ti rich side. Within the morphotropic phase compositions these local areas transformed to the monoclinic phase as temperature was decreased.

REFERENCES

[1] D. Viehland, *Phys. Rev. B* **52**, 778 (1995).

[2] X. Dai, J.-F. Li, and D. Viehland, *Phys. Rev. B* **51**, 2651 (1995).

[3] J. Ricote, D. L. Corker, R. W. Whatmore, S. A. Impey, A. M. Glazer, J. Dec, and K. Roleder, *J. Phys. Condens. Matter* **10**, 1767 (1998).

[4] D. L. Corker, A. M. Glazer, R. W. Whatmore, A. Stallard, and F. Fauth, *J. Phys. Condens. Matter* **10**, 6251 (1998).

[5] I. M. Reaney, *Proc. Electroceram.* **1**, 441 (1996).

[6] L. Bellaiche and D. Vanderbilt, *Phys. Rev. Lett.* **81**, 1318 (1998).

[7] L. Bellaiche, J. Padilla, and D. Vanderbilt, *Phys. Rev. B* **59**, 1834 (1999).

[8] B. P. Burton, *Phys. Rev. B* **59**, 6087 (1999).

[9] Z. Xu, X. Dai, and D. Viehland, *Appl. Phys. Lett.* **65**, 3287 (1994).

[10] M. El Marssi, R. Farhi, and D. Viehland, *J. Appl. Phys.* **81**, 355 (1997).

[11] M. El Marssi, R. Farhi, J.-L. Dellis, M. D. Glinchuk, L. Seguin, and D. Viehland, *J. Appl. Phys.* **83**, 5371 (1998).

[12] J. Frantti, V. Lantto, S. Nishio, and M. Kakihana, *Phys. Rev. B* **59**, 12 (1999).

[13] B. Noheda, D. E. Cox, G. Shirane, J. A. Gonzalo, L. E. Cross, R. Guo, and S.-E. Park, *Appl. Phys. Lett.* **74**, 2059 (1999).

[14] J. Frantti, V. Lantto, S. Nishio, and M. Kakihana, *Jpn. J. Appl. Phys.* **38**, 5679 (1999).

[15] J. Frantti, J. Lappalainen, S. Eriksson, V. Lantto, S. Nishio, M. Kakihana, S. Ivanov, and H. Rundlöf, *Jpn. J. Appl. Phys.* **39**, 5697 (2000).

[16] B. Noheda, J. A. Gonzalo, L. E. Cross, R. Guo, S.-E. Park, D. E. Cox, and G. Shirane, *Phys. Rev. B* **61**, 8687 (2000).

[17] J. Frantti and V. Lantto, *Phys. Rev. B* **54**, 12139 (1996).

[18] J. Frantti and V. Lantto, *Phys. Rev. B* **56**, 221 (1997).

[19] A. C. Larson and R. B. Von Dreele, *General Structure Analysis System* (LANSCE, MS-H805, Los Alamos National Laboratory, Los Alamos, NM 87545) (2000).

[20] B. Jaffe, W. R. Cook, and H. Jaffe, *Piezoelectric Ceramics* (Academic, London, 1971), p. 136.

[21] F. Jiang, S. Kojima, C. Zhao, and C. Feng, *J. Appl. Phys.* **88**, 3608 (2000).

[22] G. A. Rossetti, M. A. Rodriguez, A. Navrotsky, L. E. Cross, and R. E. Newnham, *J. Appl. Phys.* **77**, 1683 (1995).

[23] X. Dai, Z. Xu, and D. Viehland, *J. Appl. Phys.* **79**, 1021 (1996).

[24] J. M. Kiat, G. Baldinozzi, M. Dunlop, C. Malibert, B. Dkhil, C. Menorét, O. Masson, and M. T. Fernandez-Diaz, *J. Phys. Condens. Matter* **12**, 8411 (2000).

[25] C. M. Foster, Z. Li, M. Grimsditch, S.-K. Chan, and D. J. Lam, *Phys. Rev. B* **48**, 10160 (1993).

[26] Y. Ikeuchi, S. Kojima, and T. Yamamoto, *Jpn. J. Appl. Phys.* **36**, 2985 (1997).

[27] J. Frantti, *Raman studies of Nd-modified lead zirconate titanate bulk ceramics and thin films* (Acta Universitatis Ouluensis Technica **C101**, 1997), p. 54.

[28] G. Burns and B. A. Scott, *Phys. Rev. B* **7**, 3088 (1973).

[29] G. Shirane, R. Pepinsky, and B. C. Frazer, *Acta Crystallogr.* **9**, 131 (1956).

[30] L. Bellaiche, A. Garcia, and D. Vanderbilt, *Phys. Rev. Lett.* **84**, 5427 (2000).